Biogeosciences, 13, 2889–2899, 2016
www.biogeosciences.net/13/2889/2016/
doi:10.5194/bg-13-2889-2016

Biogeosciences Open Access EGU

N_2 fixation in eddies of the eastern tropical South Pacific Ocean

Carolin R. Löscher[1,2], Annie Bourbonnais[3], Julien Dekaezemacker[4,a,b], Chawalit N. Charoenpong[5,6], Mark A. Altabet[3], Hermann W. Bange[1,7], Rena Czeschel[1], Chris Hoffmann[2], and Ruth Schmitz[2]

[1]Helmholtz Center for Ocean Research Kiel, Düsternbrooker Weg 20, 24105 Kiel, Germany
[2]Institute of Microbiology, Christian Albrechts University of Kiel, Am Botanischen Garten 1–9, 24118 Kiel, Germany
[3]School for Marine Science and Technology, University of Massachusetts Dartmouth, New Bedford, Massachusetts, USA
[4]Department of Biogeochemistry, Max Planck Institute for Marine Microbiology, Celsiusstraße 1, 28359 Bremen, Germany
[5]Department of Marine Chemistry and Geochemistry, Woods Hole Oceanographic Institution, Woods Hole, Massachusetts, USA
[6]Department of Earth, Atmospheric and Planetary Sciences, Massachusetts Institute of Technology, Cambridge, Massachusetts, USA
[7]Christian Albrechts University Kiel, Christian-Albrechts-Platz 4, 24118 Kiel, Germany
[a]now at: MARUM, University of Bremen, 28359 Bremen, Germany
[b]now at: Helmholtz Young Investigator Group SEAPUMP, Alfred Wegener Institute for Polar and Marine Research, 27570 Bremerhaven, Germany

Correspondence to: C. R. Löscher (cloescher@geomar.de)

Received: 5 November 2015 – Published in Biogeosciences Discuss.: 27 November 2015
Revised: 21 April 2016 – Accepted: 29 April 2016 – Published: 18 May 2016

Abstract. Mesoscale eddies play a major role in controlling ocean biogeochemistry. By impacting nutrient availability and water column ventilation, they are of critical importance for oceanic primary production. In the eastern tropical South Pacific Ocean off Peru, where a large and persistent oxygen-deficient zone is present, mesoscale processes have been reported to occur frequently. However, investigations into their biological activity are mostly based on model simulations, and direct measurements of carbon and dinitrogen (N_2) fixation are scarce.

We examined an open-ocean cyclonic eddy and two anticyclonic mode water eddies: a coastal one and an open-ocean one in the waters off Peru along a section at 16° S in austral summer 2012. Molecular data and bioassay incubations point towards a difference between the active diazotrophic communities present in the cyclonic eddy and the anticyclonic mode water eddies.

In the cyclonic eddy, highest rates of N_2 fixation were measured in surface waters but no N_2 fixation signal was detected at intermediate water depths. In contrast, both anticyclonic mode water eddies showed pronounced maxima in N_2 fixation below the euphotic zone as evidenced by rate measurements and geochemical data. N_2 fixation and carbon (C) fixation were higher in the young coastal mode water eddy compared to the older offshore mode water eddy. A co-occurrence between N_2 fixation and biogenic N_2, an indicator for N loss, indicated a link between N loss and N_2 fixation in the mode water eddies, which was not observed for the cyclonic eddy. The comparison of two consecutive surveys of the coastal mode water eddy in November 2012 and December 2012 also revealed a reduction in N_2 and C fixation at intermediate depths along with a reduction in chlorophyll by half, mirroring an aging effect in this eddy. Our data indicate an important role for anticyclonic mode water eddies in stimulating N_2 fixation and thus supplying N offshore.

1 Introduction

Reactive nitrogen (N) limits primary production in large parts of the ocean (Codispoti, 1989). Biological dinitrogen (N_2) fixation is an important external input of N, representing more than 60–80 % of the new N provided to the Ocean (Codispoti, 2007; Duce et al., 2008), and can partially relieve N limitation. For decades, N_2 fixation was thought to occur mainly in nutrient-depleted surface waters such as those

found in the subtropical gyres (Sohm et al., 2011). However, some recent modeling studies have suggested a close spatial link between fixed N loss, i.e., N_2 production via anammox and/or denitrification, occurring in oxygen-deficient zones (ODZs), and N_2 fixation taking place in the adjacent surface ocean with the consequence that the potential habitat of N_2-fixing organisms is larger than previously thought (Deutsch et al., 2007). Furthermore, as both processes are favored under oxygen-depleted conditions and as some organisms responsible for these processes do not need light, their coupling in ODZ waters would damp excursions in the oceanic N inventory and promote the stability of the global N budget.

In recent years, efforts have been placed on investigating N_2 fixation in the eastern tropical South Pacific (ETSP; Dekaezemacker et al., 2013; Fernandez et al., 2015; Löscher et al., 2014), and the results of those field studies have significantly advanced our understanding of diazotrophy in low-O_2 regions of the ocean. Indeed, they confirmed the frequent occurrence of N_2 fixation in denitrifying waters and below the euphotic zone. The biogeochemical significance of non-cyanobacterial diazotrophs (i.e., microbes capable of N_2 fixation) has been described, and their enormous potential to fix N_2 in the ETSP seems also to depend on organic-matter supply (Fernandez et al., 2015).

In addition to its remarkable biological activities, the physically dynamic character of the ETSP in the upwelling system off Peru favors mesoscale activities (Chelton et al., 2011). Compared to other upwelling regions (e.g., off California or Benguela), enhanced frequency of eddies has been reported for this region (Chaigneau et al., 2009). Mesoscale eddies are physical structures with horizontal scales of less than 100 km and timescales of around 1 month. These features can transport physical and chemical properties from the coast towards the open ocean (Klein and Lapeyre, 2009) and impact the ocean by modulating nutrient availability (Fong et al., 2008; Altabet et al., 2012). Cyclonic and mode water eddies can inject nutrients to the euphotic zone through vertical displacement of isopycnal surfaces, which increases surface primary production (McGillicuddy et al., 2007). Overall, investigations on the impact of mesoscale eddies on N_2 fixation are scarce. Fong et al. (2008) reported a stimulation of N_2 fixation in a mode water eddy of the oligotrophic North Pacific. Another study showed increased abundances of *Trichodesmium* in mesoscale eddies of the western South and North Atlantic associated with strong temporal variations (Olson et al., 2015).

In the ODZ off Peru, mesoscale eddies have previously been identified as N loss hotspots (Altabet et al., 2012; Bourbonnais et al., 2015), but to date no detailed surveys on their relevance for N_2 fixation in this region are available. The spatial connection between N loss and N_2 fixation that has been proposed for this region (Fernandez et al., 2011) may, however, indicate a potential for N_2 fixation associated with eddies in the ODZ off Peru.

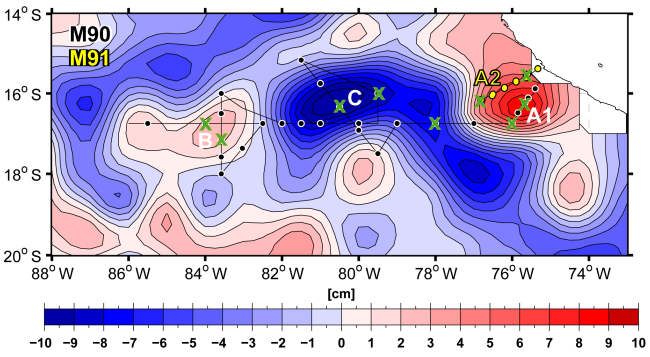

Figure 1. Distribution of AVISO satellite-derived sea surface height anomaly (SSHA) distribution as described by Stramma et al. (2013) on 21 November 2012. Eddies are labeled in white (A and B denote the coastal and the open-ocean mode water eddies, respectively; C denotes the cyclonic eddy). The cruise track from the M90 cruise is shown in black, CTD-bottle stations are indicated with black dots, green crosses denote stations sampled for N_2 fixation. The cross section through the aged coastal mode water eddy during the consecutive cruise M91 is denoted with yellow dots (A2).

The major goal of this study was to advance our understanding of eddy-related N_2 fixation by surveying one cyclonic and two anticyclonic mode water eddies along a 16.45° S transect during the R/V *Meteor* cruises M90 and M91 in November–December 2012. During the survey of these three eddies, we measured both N_2 fixation rates and abundances of *nifH*, a key functional molecular marker gene. Additionally, N_2 fixation was compared to N loss signals in the water column to investigate their coupling in the eddy systems. One particular eddy was surveyed twice (in November 2012 and December 2012), allowing the monitoring of the temporal development of N_2 fixation and primary production in an aging eddy.

2 Material and methods

2.1 Sampling description and biogeochemical parameters

Selection of sampling stations and identification of eddy cores and edges were based on sea level height anomaly data from AVISO (Archiving, Validation and Interpretation of Satellite Oceanographic data; http://aviso.altimetry.fr) and followed the criteria defined by Stramma et al. (2013). Briefly, the eddies were tracked during the R/V *Meteor* cruises M90 and M91 in November–December 2012. Three eddies were detected in area extending from the Peruvian coast to ∼ 84° W and from 15 to 18° S (Fig. 1; Stramma et al., 2013). Two eddies (further referred to as eddy A centered at about 16° S, 76° W and eddy B centered in the open ocean at about 17° S, 83° W) were mode water eddies and one was cyclonic (further referred to as eddy C, centered in

the open ocean at 16° S, 80° W; Fig. 1). The age of the eddy was determined by Stramma et al. (2013) based on satellite monitoring of sea level height anomaly data. At the time of the survey, the near-coastal eddy A was about 2 months old (3 months during the second survey), while the open-ocean eddy B was 5 months old and the cyclonic open-ocean eddy C was 2 months old.

Samples for salinity, O_2 concentrations and nutrients (nitrate, NO_3^-; nitrite, NO_2^-; phosphate, PO_4^{3-}, and ammonium, NH_4^+) were taken from a 24-Niskin-bottle rosette equipped with a conductivity–temperature–depth (CTD) sensor or from a pump CTD (Friedrich et al., 1988). O_2 concentrations were determined using a Seabird sensor, calibrated to the Winkler method (precision of 0.45 µmol L^{-1}; the lower detection limit was 2 µmol L^{-1}; Stramma et al., 2013). Nutrient concentrations were determined as previously described (Grasshoff et al., 1999) using a QuAAtro autoanalyzer (SEAL Analytical GmbH, Germany; precision for NO_2^-, NO_3^- and PO_4^{3-} was ±0.1, ±0.1 and ±0.02 µmol L^{-1}, respectively). Excess PO_4^{-3}, P* (i.e., the anomaly in P relative to expected stoichiometry with N), was calculated from dissolved inorganic nitrogen ($DIN = NO_3^- + NO_2^-$) and PO_4^{3-} measurements according to Deutsch et al. (2007):

$$P^* = PO_4^{3-} - DIN/r_{16:1}, \quad (1)$$

where $r_{16:1}$ is the ratio of nitrate to phosphate as per the Redfield stoichiometry. Positive P* has been thought to stimulate N_2 fixation

2.2 N_2 / Ar and biogenic N_2 measurements

High-precision measurements of N_2 / Ar were made on septum-sealed samples using an online gas extraction system coupled to a multicollector continuous-flow isotope-ratio mass spectrometry (IRMS) as described in Charoenpong et al. (2014). N_2 excess ($[N_2]_{excess}$), i.e., the observed $[N_2]$ minus the equilibrium $[N_2]$ at in situ temperature and salinity, was calculated based on the N_2 / Ar ratio with daily calibration against seawater standards equilibrated with air at fixed temperatures (5, 15 and 25 °C). Precision (standard deviation) for duplicate measurements was generally better than ±0.7 µmol L^{-1} for $[N_2]_{excess}$.

We calculated biogenic $[N_2]$ ($[N_2]_{biogenic}$), the $[N_2]$ produced by denitrification or anammox, by subtracting the $[N_2]_{excess}$ at a background station ($[N_2]_{excess\_bkgd}$) unaffected by N loss ($[O_2] > 10$ µmol L^{-1}) located north of the ODZ (1.67° N, 85.83° W; M90 cruise) from the observed $[N_2]_{excess}$ at corresponding σ_θ (as described in Bourbonnais et al., 2015):

$$[N_2]_{excess\_bkgd}(\mu mol\,L^{-1}) = 1 \times 10^{-9} e^{0.84.\sigma\theta}. \quad (2)$$

This corrects for nonlocal biological N loss as well as physically produced deviations in equilibrium N_2 / Ar (Hamme and Emerson, 2002).

2.3 N_2/C fixation rate measurements

Sample seawater was taken from the Niskin bottles or from the pump CTD and filled into 4.5 L polycarbonate bottles (Nalgene, Thermo Fisher, Waltham, MA, USA) capped with a Teflon-coated butyl rubber septum. Incubations were performed as previously described (Grosskopf et al., 2012) with the method developed by Mohr et al. (2010). In contrast to the traditionally used bubble addition method (Montoya et al., 1996), $^{15}N_2$ gas (Cambridge Isotopes, Lot no.: I-16727) was dissolved in degassed water from the same sampling depth in order to guarantee a high dissolution and a stable enrichment in $^{15}N_2$. Each incubation bottle was supplemented with 100 mL of $^{15}N_2$-enriched seawater containing defined amounts of 98 % $^{15}N_2$ gas in order to reach a final and constant $^{15}N_2$ enrichment of 2.4 ± 0.144 atom %. A recent study reported a slight potential contamination of $^{15}N_2$ gas with 0.024 ± 0.006 µmoles $^{15}N\text{-}NO_3^-/NO_2^-$ and 0.014 ± 0.004 µmoles $^{15}N\text{-}NH_4^+$ per mole $^{15}N_2$ (Dabundo et al., 2014). According to Dabundo et al. (2014), however, low concentrations of contaminants in Cambridge $^{15}N_2$ gas do not significantly inflate N_2 fixation rates such as those presented here. In addition, we examined the $^{15}N_2$ gas used in our incubations following the hypobromide oxidation method (Warembourg, 1993) and no contamination has been detected. For each bottle, the initial enrichment of $^{15}N_2$ has been determined and considered for the calculation of the rates.

For carbon fixation measurements, $NaH^{13}CO_3$ (98 atom % ^{13}C; Sigma-Aldrich, St. Louis; MO, USA) was dissolved in sterile MilliQ water (1 g 50 mL^{-1}). Then, 1 mL was added to the incubations with a syringe (~ 3.5 atom % final in 4.5 L bottles). In order to investigate the contribution of heterotrophic vs. autotrophic diazotrophs to N_2 fixation, glucose addition experiments were performed with ^{13}C-labeled glucose (Sigma-Aldrich, St. Louis, MO, USA), dissolved in MilliQ water (1.44 g L^{-1}), and the concentrated solution was added through the septum with a syringe to yield a final concentration of 2 µmol L^{-1} glucose. Bottles from surface water were kept in seawater-cooled on-deck Plexiglas incubators covered with blue light foil (blue-lagoon, Lee filters, Andover, Hampshire, UK) that mimics the ambient irradiance at around 10 m depth. Samples from the ODZ were stored at 12 °C in the dark. After 24 h of incubation, 0.7–2.5 L of seawater were filtered onto precombusted (450 °C, 5 h) 25 mm diameter GF/F filters (Whatman, GE healthcare, Chalfont St Giles, UK) under gentle vacuum (−200 mbar). The filtrations were stopped after 1 h since a high particle load in

surface waters often led to a clogging of the filters. Filters were oven-dried (50 °C) for 24 h and stored over desiccant until analysis. Environmental samples of 2 L untreated seawater were filtered and prepared in the same way to serve as blanks for natural abundance. For isotope analysis, GF/F filters were acidified over fuming HCl overnight in a desiccator to remove inorganic C. Filters were then oven-dried for 2 h at 50 °C and pelletized in tin cups. Samples for particulate organic carbon and nitrogen (POC and PON) and isotopic composition were analyzed on an Elemental Analyzer Flash EA 1112 series (Thermo Fisher, Waltham, MA, USA) coupled to a mass spectrometer (Finnigan Delta Plus XP, Thermo Fisher, Waltham, MA, USA). Measurements were calibrated using reference gases between each sample and caffeine every six samples. A table of N_2 and C fixation rate measurements is given in the supplementary material.

Possible correlations between environmental parameters and N_2 fixation rates were explored by principal component analysis (PCA) based on 58 cases. Computations were performed in PAST version 3.07 (Hammer et al., 2001). Metadata sets for M90 and M91were deposited at PANGAEA.

2.4 Molecular methods

For molecular analysis, nucleic acid samples were collected by filtering up to 1 L of seawater (exact volumes were recorded and the filtration time was shorter than 20 min) onto polycarbonate membrane filters with a pore size of 0.2 µm (Millipore, Darmstadt, Germany). Immediately after collection, samples were flash frozen in liquid nitrogen and stored at −80 °C until extraction. Nucleic acids were extracted using a DNA/RNA AllPrep Kit (Qiagen, Hildesheim, Germany) with minor changes in the protocol (Löscher et al., 2014).

For cDNA library construction, residual DNA was removed from the purified RNA by a DNase I treatment (Life Technologies, Carlsbad, CA, USA). The extracted RNA was gene-specifically reverse-transcribed to cDNA using the Superscript III First Strand synthesis Kit (Life Technologies, Carlsbad, CA, USA) following the manufacturers' protocol, and *nifH* cluster-specific no-template quantitative polymerase chain reactions (qPCRs) were performed to assure the purity of RNA. Quantitative PCRs were performed with cDNA as described before (Löscher et al., 2014); however, a ViiA7 qPCR system (Life Technologies, Carlsbad, CA, USA) was used and the reaction volume was reduced to 12.5 µL. The detection limit of the qPCRs was deducted from non-template controls. No amplification was detected after 45 cycles, setting the theoretical detection limit to one copy per liter. As the detection limit depends on the sample and elution volumes, we calculated a detection limit of 40 copies L^{-1}. For *nifH* transcript diversity analysis, a polymerase chain reaction (PCR) based amplification of the *nifH* gene was performed followed by Topo TA cloning and sequencing using established protocols (Lam et al., 2007; Langlois et al., 2005).

Phylogenetic analysis of *nifH* transcripts was conducted using MUSCLE (MUltiple Sequence Comparison by Log-Expectation) alignment on a 321-bp fragment with the Mega 6.0 package (Tamura et al., 2013), sequence differences were set to a minimum of 5 %, and neighbor joining trees were constructed as previously described (Löscher et al., 2014).

Table 1. Vertically integrated biogeochemical parameters of the three eddies in the ETSP during the M90 and M91 cruises. N_2 and C fixation rates as well as O_2, concentrations are expressed as integrated concentrations or abundances over the upper 500 m of the water column (data taken from the eddy centers). Chl *a* concentrations are taken from Stramma et al. (2013) and represent maximum concentrations in the subsurface maximum.

	A (M90)	A (M91)	B (M90)	C (M90)
N_2 fixation (µmol N m^{-2} d^{-1})	628.7	490.8	245.0	150.6
C fixation (mmol C m^{-2} d^{-1})	64.4	3.9	42.8	6.7
O_2 (mol m^{-2})	37.5	27.6	37.7	45.2
Chl *a* max. (µg L^{-1})	6.1	2.5	2.5	2.8

3 Results and discussion

The investigated eddies originated from the shelf–slope region of the Peru margin (however, the exact origin of eddy B could not be determined). While eddy A remained close to the coast during the 2-month period, eddies B and C propagated further offshore. Key hydrographical properties are specified below, and an extensive description can be found in Stramma et al. (2013).

Eddy A, a nearshore mode water eddy, showed a pronounced O_2 minimum from 100 m downwards with lowest concentrations close to the detection limit of the Winkler method (~ 2 µmol O_2 kg^{-1}). The influence of the coastal upwelling was visible from the lifting of the upper isopycnal towards the shore (Arévalo-Martínez et al., 2016). Below the oxycline at ~ 100 m depth, nutrient concentrations were generally higher in the ODZ relative to surface waters. While PO_4^{3-} concentrations were not considerably different in the eddy compared to surrounding waters, NO_3^- concentrations showed a pronounced decrease in the ODZ of eddy A compared to surrounding waters (see Fig. S1 in the Supplement for individual sections through eddies A, B and C). This decrease correlated with an increase in NO_2^- concentrations at the same depth ($r^2 = 0.76$, $n = 52$ below the oxycline). A comparison to biogenic N_2 as an indicator for active or past N loss processes showed a maximum along with the NO_2^- maximum, thus supporting the view of ongoing N loss in eddy A (Fig. 2; see Bourbonnais et al. (2015) for details on N loss processes in eddy A). As a result of this N loss, we observed large values for excess P*, which is typically considered to promote N_2 fixation in surface waters (Karl et al., 2002).

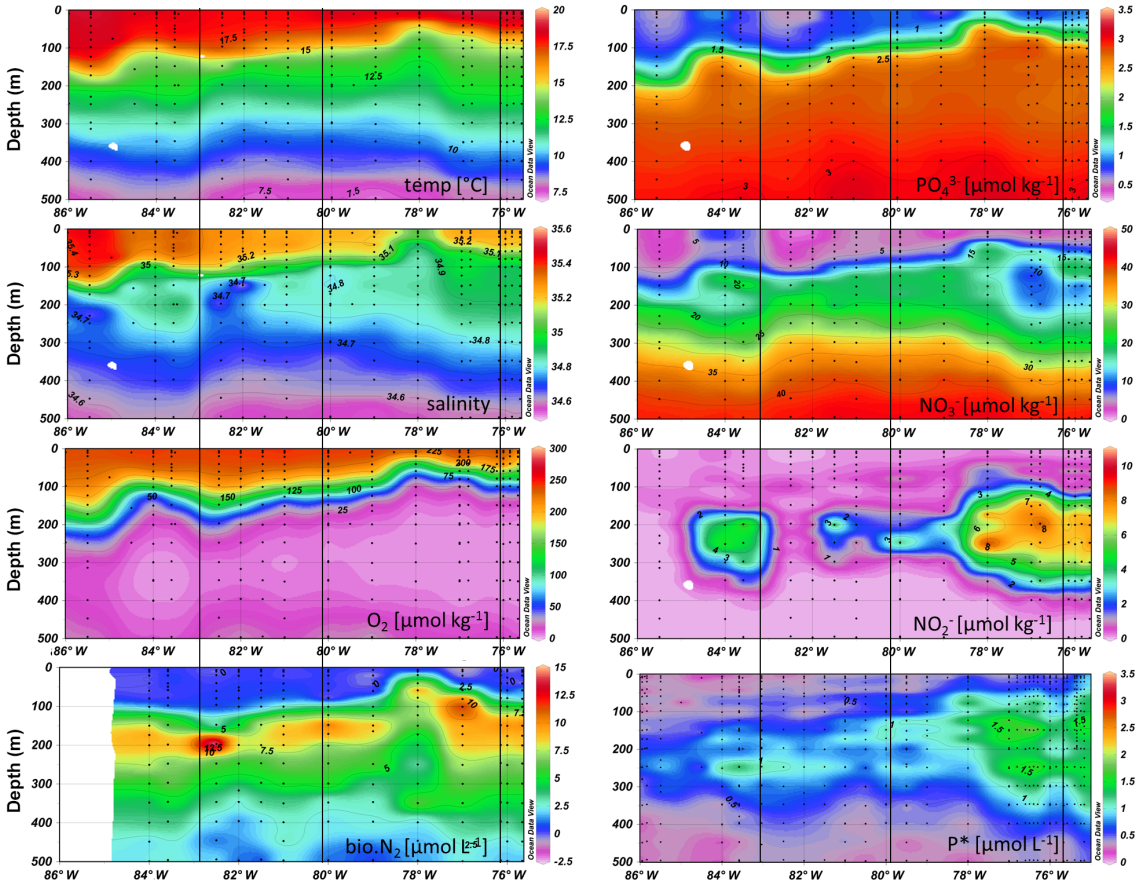

Figure 2. Temperature, salinity and oxygen, phosphate, nitrate, nitrite, biogenic N_2, and P* for eddies A, B and C along a cross section at 16°45′ S during the M90 cruise are shown. The black lines indicate the eddy centers at ∼ 76° W (eddy A), ∼ 80.1° W (eddy C) and ∼ 83.3° W (eddy B).

Eddy A, which was estimated to have been in existence for 2 months at the time of the first survey, was sampled again 1 month later; the first observation is further referred to as "eddy A1", the second survey is referred to as "eddy A2". Since the first observation, a decrease in O_2 (Table 1) and NO_3^- (Arévalo-Martínez et al., 2016; Stramma et al., 2013) has been observed, indicating ongoing respiration and N loss. These signals of enhanced ongoing N loss weakened over time as eddy A aged (Stramma et al., 2013). This may possibly be due to nutrient subduction via organic matter export out of the anticyclonic eddy (Omand et al., 2015). An extensive characterization of N loss signals in this eddy revealed a complete consumption of NO_3^- (Bourbonnais et al., 2015). The most intense N loss signals were observed near the core of eddy A, where the ODZ is in direct contact with the euphotic zone via uplifting of isopycnals (Bourbonnais et al., 2015), thus supporting the impact of freshly produced organic matter on N loss (Babbin et al., 2014).

Eddy B, an offshore mode water eddy, was characterized by slightly deeper oxycline and nutriclines compared to eddy A (at ∼ 200 m water depth). Although less pronounced than in eddy A, NO_3^- concentrations decreased within the ODZ in the eddy along with an increase in NO_2^- and biogenic N_2 between 200 and 300 m depth, again indicating N loss. P* was slightly higher in the O_2-depleted core waters, however, to a lesser extent and at slightly greater depth compared to eddy A. Stramma et al. (2013) observed weaker signals for N loss in eddy B, which were also mirrored by lower N_2O production (Arévalo-Martínez et al., 2016). This weakening may result from less organic-matter export into the core of the eddy (Fig. 2).

Eddy C was the investigated offshore cyclonic eddy (Fig. 2; Stramma et al., 2013). NO_3^- did not show the same pronounced decrease at the core of the eddy as detected in eddies A and B, but NO_2^- and biogenic N_2 were found to be slightly enriched between 200 and 300 m water depth, possibly from the onset of N loss at this location or a leftover signal from enhanced N loss within the coastal upwelling as previously described for this region (Kalvelage et al., 2013) and confirmed by the excess of P compared to N in its core waters. A coastal origin of eddy C has been described; however, compared to the mode water eddies A and B, eddy C moved

westward without staying in the shelf–slope region (Stramma et al., 2013), which may be one reason for the lower N loss signals.

3.1 Patterns of N_2 and C fixation in the three eddies

N_2 fixation was strongly associated with intermediate waters of the mode water eddies A and B, while the cyclonic eddy C showed maximum rates of N_2 fixation in surface waters but no detectable N_2 fixation in the O_2-depleted core waters.

In eddy A1, intense N_2 fixation was detected between 200 and 350 m water depth in the eddy center with maximum rates of 4.4 nmol N L^{-1} d^{-1} at 250 m depth (Fig. 3). At the same depth, carbon fixation was the highest, reaching 0.51 µmol C L^{-1} d^{-1}, coinciding with elevated N_2 fixation. High carbon fixation associated with the center of eddy A, however, extended deeper down to 400 m. High carbon fixation in the absence of light (compare chl a data in Stramma et al., 2013) is likely attributed to dark carbon fixation as previously described as taking place in this and other oxygen minimum zones (Schunck et al., 2013; Taylor et al., 2010). Similarly, eddy B showed high rates of N_2 fixation at its center, with a maximum of 1.89 nmol N L^{-1} d^{-1} at 350 m depth. In eddy B, the maximum in carbon fixation was exclusively present above the upper isopycnal (between 100 and 200 m; Stramma et al., 2013) and thus not in direct contact with the N_2 fixation zone. However, a smaller peak could be observed at $\sim$ 380 m depth. Maximum N_2 fixation rates in eddy C (0.51–1.48 nmol N L^{-1} d^{-1}) were detected in surface waters (Table S1 in the Supplement). Carbon fixation in eddy C was lower compared to eddy A and eddy B; however, it was detectable in all samples.

Compared to previous studies in this area, N_2 fixation rates for eddies A and B are generally 1–2 orders of magnitude higher (e.g., Dekaezemacker et al. (2013): 0.01–0.88 nmol N L^{-1} d^{-1}; Löscher et al. (2014): 0.01–0.4 nmol N L^{-1} d^{-1}); here, it must be noted that we used the improved method by Mohr et al. (2010), which allows us to present here the first quantitative rates of N_2 fixation in this area, while previous studies may have underestimated N_2 fixation rates (Grosskopf et al., 2012). An aging effect was mirrored by a decrease in N_2 and C fixation below 200 m at the center of Eddy A when comparing the measurements from eddy A1 sampled in November 2012 with eddy A2 surveyed a month later in December 2012. C fixation rates increased towards the eddy edge. This may be attributed to biological consumption or the export of nutrients needed for biological activities within the eddy that are still available due to lower consumption or diffusion through the rim.

Observations of higher N_2 fixation rates in accordance with our data set suggest an overall stimulation of N_2 fixation associated with anticyclonic mode water eddies (Fong et al., 2008). N_2 fixation rates of 8.6 nmol N L^{-1} d^{-1} have been measured in the surface waters of an eddy in the oligotrophic North Pacific Ocean (Fong et al., 2008). N_2 fixation was only measured in surface water samples (5 m depth) by Fong et al. (2008); thus, a direct comparison with N_2 fixation within the O_2-depleted eddy core waters, as measured in this study, is not possible.

The occurrence of enhanced N_2 fixation associated with intermediate water depths is in accordance with our previous study from that region, where we detected a variety of non-cyanobacterial diazotrophs compared to relatively minor numbers of cyanobacterial diazotrophs related to *Crocosphaera* (Löscher et al., 2014). In order to characterize the expression of the key functional marker gene for N_2 fixation, *nifH*, we conducted a phylogenetic study on *nifH* diversity in the transcript pool. Similar to the previous study, most of the detected *nifH* transcripts were affiliated to non-cyanobacterial diazotrophs (P1-P8) with some cyanobacterial *Crocosphaera*-related (UCYN-B) *nifH* sequences present to a much lesser extent (Fig. 4, Table S2). Quantification of *nifH* transcripts related to the detected clusters showed maximum abundances associated with the maxima in N_2 fixation in eddies A, B and C (Fig. 4). A potential for heterotrophic N_2 fixation was deducted from glucose fertilization experiments with water samples from the cores of eddies A and B. Here, glucose addition greatly enhanced N_2 fixation from 0.86 ± 0.1 to 39.19 ± 4.31 nmol N L^{-1} d^{-1} at 100 m depth in eddy A and from 0.251 ± 0.03 to 62.18 ± 1.9 nmol N L^{-1} d^{-1} at 125 m depth in eddy B. However, no increase in N_2 fixation by glucose addition could be achieved in eddy C (100 m, Fig. 5), which may result from different diazotrophic communities (i.e., cyanobacterial UCYN-B *nifH* sequences present). Therefore, the availability of reduced carbon compounds may essentially control N_2 fixation in mode water eddies. Assuming that organic-matter export is limiting for N loss as previously suggested (Babbin et al., 2014; Ogawa et al., 2001; Bianchi et al., 2014) and that deep-water N_2 fixation is a non-cyanobacterial (i.e., heterotrophic) process as shown by the diversity of the diazotrophs and the stimulation of N_2 fixation rates after glucose addition, the interplay between both may be even closer than previously thought.

3.2 Co-occurrence of N_2 fixation and N loss in mode water eddies

Largely consistent with the distribution of NO_2^-, biogenic N_2 showed pronounced maxima below the mixed layer depth in eddies A and B and a less pronounced maximum in eddy C. A similar distribution has been determined for P* (Fig. 2). The consistency of those parameters indicates either ongoing N loss or its leftover signal as already reported for the upwelling off Peru (Kalvelage et al., 2013). In an earlier study from that region (i.e., Löscher et al., 2014), we found a close spatial coupling between N loss, or a relic signal as suggested by Kalvelage et al. (2013), and N_2 fixation for the same upwelling region off Peru. The strongest signals for both N_2 fixation and N loss were tightly linked to a coastal sulfidic

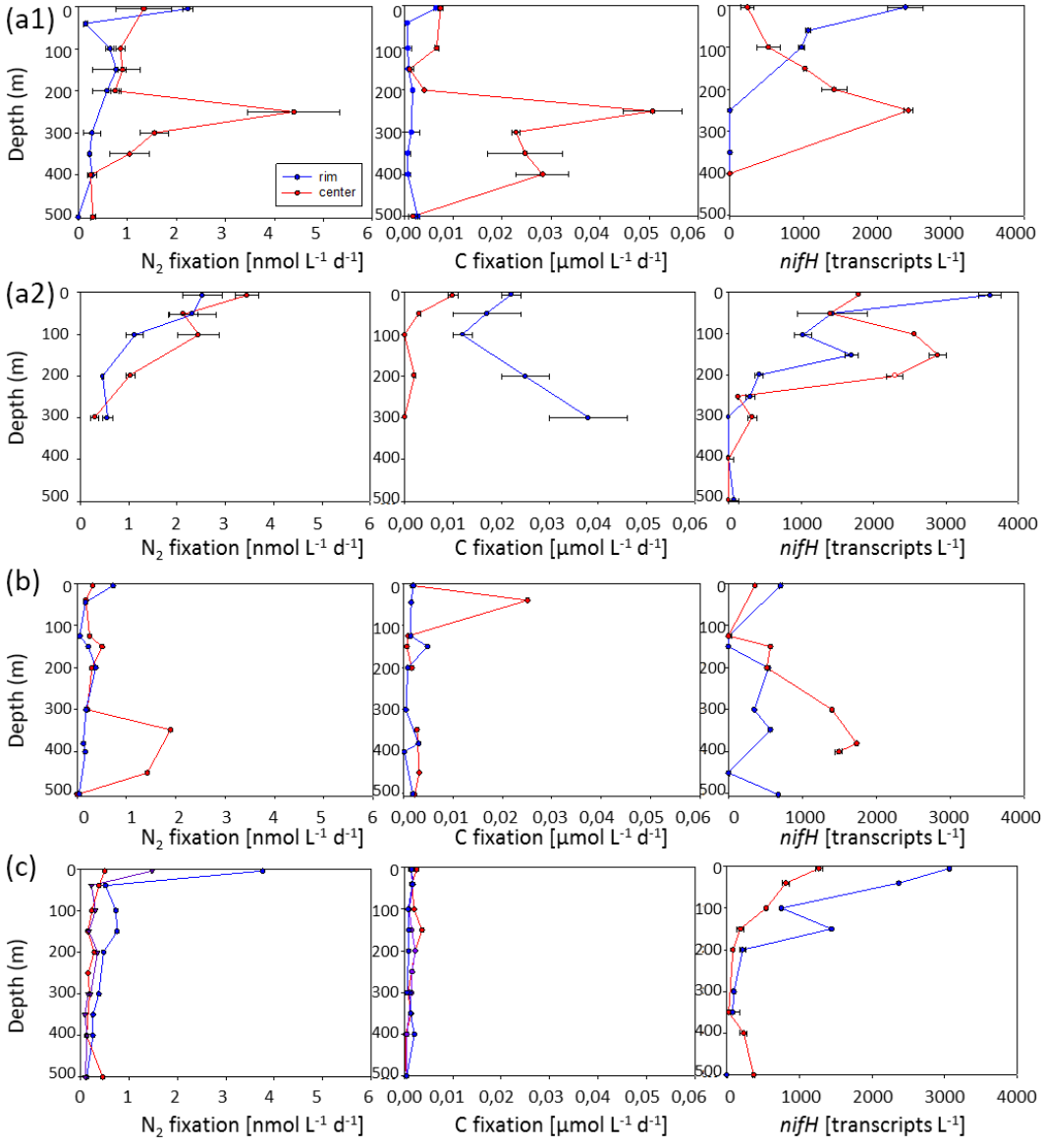

Figure 3. Vertical distributions of N_2 and C fixation rates and *nifH* transcript abundance (sum of detected clusters P2, P7 and *Crocosphaera*-like diazotrophs as quantified by qPCR) in eddy A1 (M90) (**a1**), eddy A2 (M91) (**a2**), eddy B (**b**) and eddy C (**c**).

plume (Schunck et al., 2013). The westward propagation of mesoscale eddies implies that properties of the waters which were "trapped" within its center at the time of formation are transported offshore (Chelton et al., 2007). Enhanced N_2 and C fixation rates, as well as a high N deficit, as depicted by P^*, and biogenic N_2 concentrations in eddy B indeed suggest that this coupling can be transported far offshore.

A coupling between N loss and N_2 fixation is indicated by (i) the concurrent deepening of the maxima in N loss (i.e., maximum in biogenic N_2) and N_2 fixation from the coast to the open ocean, (ii) the concurrent decrease in both biogenic N_2 concentrations and N_2 fixation rates over time and (iii) the co-occurrence between NO_2^- (either resulting from NO_3^- reduction or from the remineralization of organic matter through NH_4^+ oxidation) and N_2 fixation rates and between biogenic N_2 and N_2 fixation rates (Figs. 2, 3). We observed lower biogenic N_2 signals and N_2 fixation in eddy B compared to eddy A1 with the maximum in N_2 fixation located deeper ($\sim$ 350 m) in the water column compared to eddy A1 ($\sim$ 250 m). While we detected enhanced carbon fixation in eddy A at the same depth as N_2 fixation, this coupling was far less pronounced in eddy B. Still P^* was lower in eddy B compared to eddy A, which points towards a normalization of the N : P ratio via N_2 fixation.

Although, our results provide evidence for a coupling of N_2 fixation and N loss, statistical analysis of our data set did

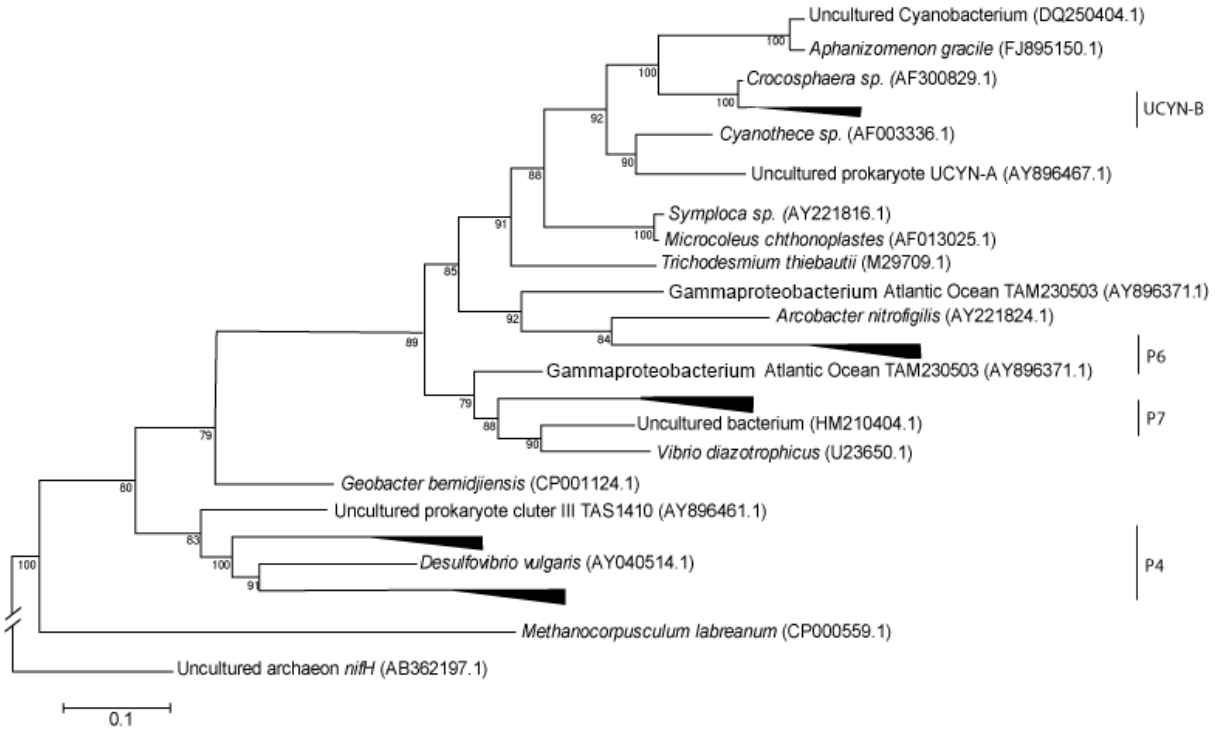

Figure 4. Phylogenetic diversity in *nifH* cDNA libraries. Black triangles denote detected clusters present in samples from M90 and M91. The tree was constructed from a ClustalW alignment as a neighbor joining tree; bootstrap values are given (% of 1000 bootstraps) below branches; P4, P6 and P7 are clusters previously identified in that region (Löscher et al., 2014).

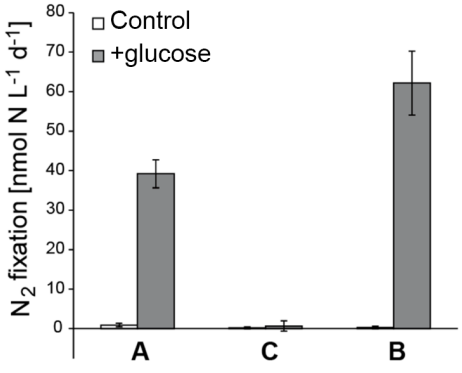

Figure 5. N_2 fixation in response to glucose fertilization experiment performed in eddies A1 (100 m), B (125 m) and C (100 m); samples were derived from the eddy core waters; depths are given in brackets.

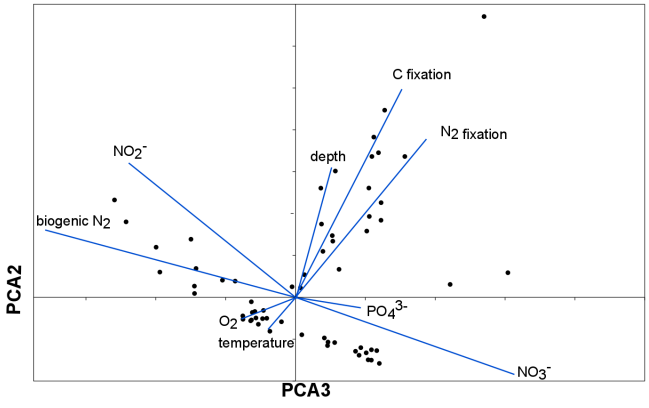

Figure 6. Principal component analysis correlation biplot showing relations between N_2 fixation and environmental variables. Strongest negative correlations are present between N_2 fixation and O_2 and between N_2 fixation and temperature. N_2 fixation is positively correlated with C fixation as indicated by the direction of vectors. Black dots denote single samples ($n = 58$).

not confirm N loss as an exclusive control on N_2 fixation but displays a dependence of N_2 fixation on O_2 and temperature (Fig. 6). The dependency on O_2 would explain the difference in N_2 fixation between the mode water eddies A and B and the cyclonic eddy C, which was slightly less anoxic in its ODZ. Several studies suggested primary production to be limited by Fe availability in the upwelling system off Peru (Bruland et al., 2005; Hutchins et al., 2002; Messie and Chavez, 2015). In their study from the same cruise series, Baker et al. (2016) report an excess Fe supply (with respect to N supply) via atmospheric deposition to the southern part of this region (∼ 15–16° S). As previous studies identified iron (Fe) to generally (co-)limit N_2 fixation (Mills et al., 2004;

Moore and Doney, 2007; Moore et al., 2009), atmospheric Fe sources may promote surface water N_2 fixation, which may explain enhanced N_2 fixation in the surface waters of the eddies. Other studies emphasize the comparably higher importance of the benthic Fe source in these waters (Chever et al., 2015; Scholz et al., 2014), which may be particularly important in eddies A and B due to their longer residence time at the coast. Enhanced N_2 fixation in the mode-water eddies A and B may, besides a coupling to N loss, also be promoted by Fe availability, possibly from benthic sources.

4 Conclusions

We conducted the first detailed survey of N_2 fixation in three eddies off the coast of Peru in the ETSP. Our results demonstrated enhanced N_2 fixation rates connected to two anticyclonic mode water eddies off Peru, while elevated N_2 fixation was not observed in the cyclonic eddy. N_2 fixation rates were highest in the ODZ of the two anticyclonic mode water eddies. This is in agreement with recent findings, which demonstrated that N_2 fixation is not only present in oligotrophic surface waters but also widely distributed throughout the water column. N_2 fixation co-occurred with N loss processes, which in combination with low O_2 concentrations may largely explain the presence of N_2 fixation in ODZ waters. Taken together, our results point towards an important role for eddies in supplying fixed N compounds to the open ocean via enhanced N_2 fixation. Although our data do not allow quantification of the overall impact of eddies on N_2 fixation in the ETSP off Peru, they clearly underscore the importance of high-resolution surveys for understanding the biogeochemistry of N cycle processes in eddies.

Data availability

Gene sequences were submitted to the National Center for Biotechnology Information (NCBI), accession numbers KX090448-KX090515. Biogeochemical data sets are available from Pangaea (Bange, 2013a, b; Krahmann, 2014; Stramma and Lohmann, 2016).

The Supplement related to this article is available online at doi:10.5194/bg-13-2889-2016-supplement.

Acknowledgements. We thank the Peruvian authorities for the permission to work in their territorial waters. We further thank the captains, crews and chief scientists of R/V *Meteor* during the M90 and M91 cruises. We acknowledge the technical assistance of T. Baustian, V. Len, V. Lohmann, N. Martogli, G. Krahmann, K. Nachtigall, M. Philippi, H. Schunck and J. Larkum. We further thank L. Stramma, D. Arevalo-Martinez, S. Thomsen, C. Callbeck and J. Karstensen for helpful discussion of the results. The cruise M91 was funded by the BMBF project SOPRAN with grant no. FKZ 03F0662A. This study is a contribution of the DFG-supported collaborative research center SFB754 (http://www.sfb754.de) and was supported by NSF grants OCE 0851092 and OCE 115474 to M. A. Altabet and an NSERC Postdoctoral Fellowship to A. Bourbonnais.

Edited by: S. W. A. Naqvi

References

Altabet, M. A., Ryabenko, E., Stramma, L., Wallace, D. W. R., Frank, M., Grasse, P., and Lavik, G.: An eddy-stimulated hotspot for fixed nitrogen-loss from the Peru oxygen minimum zone, Biogeosciences, 9, 4897–4908, doi:10.5194/bg-9-4897-2012, 2012.

Arévalo-Martínez, D. L., Kock, A., Löscher, C. R., Schmitz, R. A., Stramma, L., and Bange, H. W.: Influence of mesoscale eddies on the distribution of nitrous oxide in the eastern tropical South Pacific, Biogeosciences, 13, 1105–1118, doi:10.5194/bg-13-1105-2016, 2016.

Babbin, A. R., Keil, R. G., Devol, A. H., and Ward, B. B.: Organic matter stoichiometry, flux, and oxygen control nitrogen loss in the Ocean, Science, 344, 406–408, doi:10.1126/science.1248364, 2014.

Bange, H. W.: Oxygen measured on water bottle samples during METEOR cruise M91, GEOMAR – Helmholtz Centre for Ocean Research Kiel, doi:10.1594/PANGAEA.817193, 2013a.

Bange, H. W.: Nutrients measured on water bottle samples during METEOR cruise M91, GEOMAR – Helmholtz Centre for Ocean Research Kiel, doi:10.1594/PANGAEA.817174, 2013b.

Baker, A. R., Thomas, M., Bange, H. W., and Plasencia Sánchez, E.: Soluble trace metals in aerosols over the tropical southeast Pacific offshore of Peru, Biogeosciences, 13, 817–825, doi:10.5194/bg-13-817-2016, 2016.

Bianchi, D., Babbin, A. R., and Galbraith, E. D.: Enhancement of anammox by the excretion of diel vertical migrators, P. Natl. Acad. Sci. USA, 111, 15653–15658, doi:10.1073/pnas.1410790111, 2014.

Bourbonnais, A., Altabet, M. A., Charoenpong, C. N., Larkum, J., Hu, H., Bange, H. W., and Stramma, L.: N-loss isotope effects in the Peru oxygen minimum zone studied using a mesoscale eddy as a natural tracer experiment, Global Biogeochem. Cy., 29, 793–811, doi:10.1002/2014GB005001, 2015.

Bruland, K. W., Rue, E. L., Smith, G. J., and DiTullio, G. R.: Iron, macronutrients and diatom blooms in the Peru upwelling regime: brown and blue waters of Peru, Mar. Chem., 93, 81–103, 2005.

Chaigneau, A., Eldin, G., and Dewitte, B.: Eddy activity in the four major upwelling systems from satellite altimetry (1992–2007), Prog. Oceanogr., 83, 117–123, 2009.

Charoenpong, C. N., Bristow, L. A., and Altabet, M. A.: Dissolved gases are powerful tracers for physical and biogeochemical processes in aquatic systems, Limnol. Oceanogr.-Methods, 12, 323–337, doi:10.4319/lom.2014.12.32. ,2014.

Chelton, D. B., Schlax, M. G., Samelson, R. M., and de Szoeke, R. A.: Global observations of large oceanic eddies, Geophys. Res. Lett., 34, L15606, doi:10.1029/2007GL030812, 2007.

Chelton, D. B., Gaube, P., Schlax, M. G., Early, J. J., and Samelson, R. M.: The Influence of Nonlinear Mesoscale Eddies on Near-Surface Oceanic Chlorophyll, Science, 334, 328–332, 2011.

Chever, F., Rouxel, O. J., Croot, P. L., Ponzevera, E., Wuttig, K., and Auro, M.: Total dissolvable and dissolved iron isotopes in the water column of the Peru upwelling regime, Geochim. Cosmochim. Ac., 162, 66–82, doi:0.1016/j.gca.2015.04.031, 2015.

Codispoti, L. A.: Phosphorus vs. nitrogen limitation of new and export production, in: Productivity of the Ocean: Present and Past, edited by: Berger, H., Smetacek, V. S., and Wefer, G., John Wiley & Sons, New York, 377–394, 1989.

Codispoti, L. A.: An oceanic fixed nitrogen sink exceeding 400 $Tg\,N\,a^{-1}$ vs. the concept of homeostasis in the fixed-nitrogen inventory, Biogeosciences, 4, 233–253, doi:10.5194/bg-4-233-2007, 2007.

Dabundo, R., Lehmann, M. F., Treibergs, L., Tobias, C. R., Altabet, M. A., Moisander, P. H., and Granger, J.: The Contamination of Commercial $^{15}N_2$ Gas Stocks with ^{15}N–Labeled Nitrate and Ammonium and Consequences for Nitrogen Fixation Measurements, PLoS One, 9, e110335, doi:10.1371/journal.pone.0110335, 2014.

Dekaezemacker, J., Bonnet, S., Grosso, O., Moutin, T., Bressac, M., and Capone, D. G.: Evidence of active dinitrogen fixation in surface waters of the eastern tropical South Pacific during El Nino and La Nina events and evaluation of its potential nutrient controls, Global Biogeochem. Cy., 27, 768–779, doi:10.1002/gbc.20063, 2013.

Deutsch, C., Sarmiento, J. L., Sigman, D. M., Gruber, N., and Dunne, J. P.: Spatial coupling of nitrogen inputs and losses in the ocean, Nature, 445, 163–167, doi:10.1038/nature05392, 2007.

Duce, R. A., LaRoche, J., Altieri, K., Arrigo, K. R., Baker, A. R., Capone, D. G., Cornell, S., Dentener, F., Galloway, J., Ganeshram, R. S., Geider, R. J., Jickells, T., Kuypers, M. M., Langlois, R., Liss, P. S., Liu, S. M., Middelburg, J. J., Moore, C. M., Nickovic, S., Oschlies, A., Pedersen, T., Prospero, J., Schlitzer, R., Seitzinger, S., Sorensen, L. L., Uematsu, M., Ulloa, O., Voss, M., Ward, B., and Zamora, L.: Impacts of atmospheric anthropogenic nitrogen on the open ocean, Science, 320, 893–897, doi:10.1126/science.1150369, 2008.

Fernandez, C., Farias, L., and Ulloa, O.: Nitrogen Fixation in Denitrified Marine Waters, Plos One, 6, e20539, doi:10.1371/journal.pone.0020539, 2011.

Fernandez, C., Gonzalez, M. L., Muñoz, C., Molina, V., and Farias, L.: Temporal and spatial variability of biological nitrogen fixation off the upwelling system of central Chile (35–38.5° S), J. Geophys. Res.-Oceans, 120, 3330–3349, doi:10.1002/2014JC010410, 2015.

Fong, A. A., Karl, D. M., Lukas, R., Letelier, R. M., Zehr, J. P., and Church, M. J.: Nitrogen fixation in an anticyclonic eddy in the oligotrophic North Pacific Ocean, ISME J., 2, 663–676, doi:10.1038/ismej.2008.22, 2008.

Friedrich, G. E., Codispoti, L. A., and Sakamoto, C. M.: Bottle and pumpcast Data from the 1988 Black Sea Expedition, MBARI, Pacific Grove, Monterey, CA 93950, USA, Technical Report, 1988.

Grasshoff, G., Kremling, K., and Erhardt, M. : Methods of seawater analysis, 3 Edn., Wiley VCH, Weinheim, 1999.

Grosskopf, T., Mohr, W., Baustian, T., Schunck, H., Gill, D., Kuypers, M. M. M., Lavik, G., Schmitz, R. A., Wallace, D. W. R., and LaRoche, J.: Doubling of marine dinitrogen-fixation rates based on direct measurements, Nature, 488, 361–364, doi:10.1038/nature11338, 2012.

Hamme, R. C. and Emerson, S. R.: Mechanisms controlling the global oceanic distribution of the inert gases argon, nitrogen and neon, Geophys. Res. Lett., 29, 2120, doi:10.1029/2002GL015273, 2002.

Hammer, Ø., Harper, D. A. T., and Ryan, P. D.: PAST: Paleontological statistics software package for education and data analysis, Palaeontologia Electronica, 4, 9 pp., 2001.

Hutchins, D. A., Hare, C. E., Weaver, R. S., Zhang, Y., Firme, G. F., DiTullio, G. R., Alm, M. B., Riseman, S. F., Maucher, J. M., Geesey, M. E., Trick, C. G., Smith, G. J., Rue, E. L., Conn, J., and Bruland, K. W: Phytoplankton iron limitation in the Humboldt Current and Peru Upwelling, Limnol. Oceanogr., 47, 997–1011, 2002.

Kalvelage, T., Lavik, G., Lam, P., Contreras, S., Artega, L., Löscher, C. R., Oschlies, A., Paulmier, A., Stramma, L., and Kuypers, M. M. M.: Nitrogen cycling driven by organic matter export in the South Pacific oxygen minimum zone, Nat. Geosci., 6, 228–234, 2013.

Karl, D., Michaels, A., Bergman, B., Capone, D., Carpenter, E., Letelier, R., Lipschultz, F., Paerl, H., Sigman, D., and Stal, L.: Dinitrogen fixation in the world's oceans, Biogeochemistry, 57, 47–98, 2002.

Klein, P., and Lapeyre, G.: The Oceanic Vertical Pump Induced by Mesoscale and Submesoscale Turbulence, in: Annual Review of Marine Science, Annu. Rev. Mar. Sci., 351-375, 2009.

Krahmann, G.: Physical oceanography during METEOR cruise M90, GEOMAR – Helmholtz Centre for Ocean Research Kiel, doi:10.1594/PANGAEA.830245, 2014.

Lam, P., Jensen, M. M., Lavik, G., McGinnis, D. F., Muller, B., Schubert, C. J., Amann, R., Thamdrup, B., and Kuypers, M. M. M.: Linking crenarchaeal and bacterial nitrification to anammox in the Black Sea, P. Natl. Acad. Sci. USA, 104, 7104–7109, doi:10.1073/pnas.0611081104, 2007.

Langlois, R. J., LaRoche, J., and Raab, P. A.: Diazotrophic diversity and distribution in the tropical and subtropical Atlantic ocean, Appl. Environ. Microbiol., 71, 7910–7919, doi:10.1128/aem.71.12.7910-7919.2005, 2005.

Löscher, C. R., Großkopf, T., Desai, F., Gill, D., Schunck, H., Croot, P., Schlosser, C., Neulinger, S. C., Lavik, G., Kuypers, M. M. M., LaRoche, J., and Schmitz, R. A.: Facets of diazotrophy in the oxygen minimum zone off Peru, ISME J., 8, 2180–2192, doi:10.1038/ismej.2014.71, 2014.

McGillicuddy, D. J., Anderson, L. A., Bates, N. R., Bibby, T., Buesseler, K. O., Carlson, C. A., Davis, C. S., Ewart, C., Falkowski, P. G., Goldthwait, S. A., Hansell, D. A., Jenkins, W. J., Johnson, R., Kosnyrev, V. K., Ledwell, J. R., Li, Q. P., Siegel, D. A., and Steinberg, D. K.: Eddy/wind interactions stimulate extraordinary mid-ocean plankton blooms, Science, 316, 1021–1026, doi:10.1126/science.1136256, 2007.

Messie, M. and Chavez, F. P.: Seasonal regulation of primary production in eastern boundary upwelling systems, Prog. Oceanogr., 134, 1–18, doi:10.1016/j.pocean.2014.10.011, 2015.

Mills, M. M., Ridame, C., Davey, M., La Roche, J., and Geider, J. G.: Iron and phosphorus co-limit nitrogen fixation in the eastern tropical North Atlantic, Nature, 429, 292–294, doi:10.1038/nature02550, 2004.

Mohr, W., Grosskopf, T., Wallace, D. W. R., and LaRoche, J.: Methodological underestimation of oceanic nitrogen fixation rates, PLoS One, 5, e12583, doi:10.1371/journal.pone.0012583, 2010.

Montoya, J. P., Voss, M., Kahler, P., and Capone, D. G.: A simple, high-precision, high-sensitivity tracer assay for N_2 fixation, Appl. Environ. Microbiol., 62, 986–993, 1996.

Moore, J. K. and Doney, S. C.: Iron availability limits the ocean nitrogen inventory stabilizing feedbacks between marine denitrification and nitrogen fixation, Global Biogeochem. Cy., 21, GB2001, doi:10.1029/2006GB002762, 2007.

Moore, M. C., Mills, M. M., Achterberg, E. P., Geider, R. J., LaRoche, J., Lucas, M. I., McDonagh, E. L., Pan, X., Poulton, A. J., Rijkenberg, M. J. A., Suggett, D. J., Ussher, S. J., and Woodward, E. M. S.: Large-scale distribution of Atlantic nitrogen fixation controlled by iron availability, Nat. Geosci., 2, 867–871, 2009.

Ogawa, H., Amagai, Y., Koike, I., Kaiser, K., and Benner, R.: Production of refractory dissolved organic matter by bacteria, Science, 292, 917–920, doi:10.1126/science.1057627, 2001.

Olson, E. M., McGillicuddy, D. J., Flierl, G. R., Davis, C. S., Dyhrman, S. T., and Waterbury, J. B.: Mesoscale eddies and Trichodesmium spp. distributions in the southwestern North Atlantic, J. Geophys. Res.-Oceans, 120, 4129–150, doi:10.1002/2015JC010728, 2015.

Omand, M. M., D'Asaro, E. A., Lee, C. M., Perry, M. J., Briggs, N., Cetinić, I., and Mahadevan, A.: Eddy-driven subduction exports particulate organic carbon from the spring bloom, Science, 348, 222–225, doi:10.1126/science.1260062, 2015.

Scholz, F., McManus, J., Mix, A. C., Hensen, C., and Schneider, R. R.: The impact of ocean deoxygenation on iron release from continental margin sediments, Nat. Geosci., 7, 433–437, 2014.

Schunck, H., Lavik, G., Desai, D. K., Großkopf, T., Kalvelage, T., Löscher, C. R., Paulmier, A., Contreras, S., Siegel, H., Holtappels, M., Rosenstiel, P., Schilhabel, M. B., Graco, M., Schmitz, R. A., Kuypers, M. M. M., and LaRoche, J.: Giant Hydrogen Sulfide Plume in the Oxygen Minimum Zone off Peru Supports Chemolithoautotrophy, PLoS ONE, 8, e68661, doi:10.1371/journal.pone.0068661, 2013.

Sohm, J. A., Webb, E. A., and Capone, D. G.: Emerging patterns of marine nitrogen fixation, Nat. Rev. Microbiol., 9, 499–508, 2011.

Stramma, L. and Lohmann, M.: Hydrochemistry of water samples during METEOR cruise M90, doi:10.1594/PANGAEA.857751, 2016.

Stramma, L., Bange, H. W., Czeschel, R., Lorenzo, A., and Frank, M.: On the role of mesoscale eddies for the biological productivity and biogeochemistry in the eastern tropical Pacific Ocean off Peru, Biogeosciences, 10, 7293–7306, doi:10.5194/bg-10-7293-2013, 2013.

Tamura, K., Stecher, G., Peterson, D., Filipski, A., and Kumar, S.: MEGA6: Molecular Evolutionary Genetics Analysis Version 6.0, Mol. Biol. Evol., 30, 2725–2729, 2013.

Taylor, G. T., Iabichella, M., Ho, T.-Y., Scranton, M. I., Thunell, R. C., Muller-Karger, F., and Varela, R.: Chemoautotrophy in the redox transition zone of the Cariaco Basin: A significant midwater source of organic carbon production, Limnol. Oceanogr., 46, 148–163, doi:10.4319/lo.2001.46.1.0148, 2010.

Warembourg, F. R.: Nitrogen fixation in soil and plant systems, in: Nitrogen Isotope Techniques, edited by: Knowles, R. and Blackburn, T. H., Academic Press, San Diego, USA, 127–156, 1993.